



1 **Sea surface salinity and temperature in the Southern Atlantic**
2 **Ocean from South African icebreakers, 2010–2017**

3
4 Giuseppe Aulicino^{1,2}, Yuri Cotroneo², Isabelle Ansoerge³, Marcel van den Berg⁴, Cinzia Cesarano⁵,
5 Maria Belmonte Rivas^{6,7}, Estrella Olmedo Casal⁶

6
7 ¹ Department of Life and Environmental Sciences, Università Politecnica delle Marche, Ancona, 60131, Italy

8 ² Department of Science and Technologies, Università degli studi di Napoli Parthenope, Napoli, 80143, Italy

9 ³ Marine Research Institute, Oceanography Department, University of Cape Town, Rondebosch, 7701, South Africa

10 ⁴ Department of Environmental Affairs, Cape Town, 8001, South Africa

11 ⁵ Progetto Terra, Gragnano, 80054, Italy

12 ⁶ Institute of Marine Sciences, ICM, Barcelona, 08003, Spain

13 ⁷ Royal Netherlands Meteorological Institute, KNMI, De Bilt, 3730, Netherlands

14

15 *Correspondence to:* Giuseppe Aulicino (g.aulicino@staff.univpm.it)

16

17 **Abstract.** We present here sea surface salinity (SSS) and temperature (SST) data collected onboard the SA Agulhas-I
18 and SA Agulhas-II research vessels, in the framework of the South African National Antarctic Programme (SANAP).
19 Onboard SeaBird ThermoSalinoGraphs were regularly calibrated and continuously monitored in-between cruises, and
20 no appreciable sensor drift emerged. Water samples were taken on a daily basis and later analysed with a Portasal
21 salinometer; some-CTD measurements collected along the cruises were used to validate the data. No systematic
22 differences appeared after a rigorous quality control on continuous data. Results show that salinity measurement error
23 was a few hundredths of a unit on the practical salinity scale. Quality control included several steps, among which an
24 automatic detection of unreliable values through selected thresholds criteria and an attribution of quality flags based on
25 multiple criteria, i.e. analysis of information included in the cruise reports, detection of insufficient flow and/or
26 presence of air bubbles in the seawater pipe, visual inspection of individual campaigns, ex-post check of seaice maps
27 for confirming icefields locations. This data processing led to discard about 36 % of acquired observations, while
28 reliable data showed an excellent agreement with several independent SSS products. Nevertheless, a seaice flag has
29 been included for identifying valid data which could have been affected by scattered seaice contamination. In our
30 opinion this dataset, available through an unrestricted repository at <https://doi.org/10.7289/V56M3545>, contributes to
31 improve the knowledge of surface water features in one of the most important regions for global climate. That will be
32 highly valuable for studies focusing on climate variability in the Atlantic sector of the Southern Ocean, especially
33 across the Antarctic Circumpolar Current and its fronts. Furthermore, we expect that the collected SSS will represent a
34 valuable tool for the calibration and validation of recent satellite observations provided by SMOS and Aquarius
35 missions.

36



37 1 Introduction

38 The salinity of the ocean is one of the key parameters identified by the Global Climate Observing System (GCOS) as
39 being essential for climate studies (World Meteorological Organization, 2016). Many water masses are identified and
40 traced through salinity values; in addition, the entire ocean circulation from surface to deep layers is largely conditioned
41 by their influence on the density field (e.g., Rahmstorf, 2006; Helm et al., 2010; Sansiviero et al., 2017). Increasing
42 efforts have been made in the past decades to provide a global synoptic monitoring of the sea surface salinity (SSS) in
43 conjunction with the recent launch of two dedicated satellite missions, i.e. SMOS in 2009 (Kerr et al, 2010) and
44 Aquarius in 2011 (Le Vine et al., 2010). The delivered remote sensed data provided interesting insights into the upper
45 ocean, especially when considering that the surface layer is strictly connected to i) the physical and biogeochemical
46 interactions between ocean and atmosphere and ii) the observation of large-scale circulation features (i.e., fronts,
47 currents) as well as mesoscale and small-scale structures (i.e., meanders, eddies) (Cotroneo et al., 2013; Reul et al.,
48 2014; D'Addezio and Subrahmanyam, 2016). Nevertheless, original SMOS and Aquarius products showed limitations
49 in retrieving completely reliable SSS values in some regions of the worldwide oceans, especially at latitudes higher than
50 45-50° (Tang et al., 2014; Kohler et al., 2015). Despite their oceanographic and biological importance, the southern
51 sector of the Atlantic Ocean and the correspondent sector of the Southern Ocean are among such areas. It is recognized
52 by the scientific community that further studies are needed to improve the satellite SSS retrievals calibration and
53 validation in these regions (Lagerloef et al., 2010; Chen et al., 2014; Boutin et al., 2016). To this aim, all the available
54 near surface measurements (mostly in the upper five meters) are welcome and should be shared by the oceanographic
55 community.

56 Since 2010, South Africa's Department of Environmental Affairs (DEA), the South African National Antarctic
57 Programme (SANAP) and the University of Cape Town (UCT) have carried out annual research cruises across the
58 Southern Ocean, as part of the SAMOC-SA programme (Ansorge et al., 2014), in order to collect multidisciplinary
59 meteo-oceanographic in situ data.

60 ThermoSalinoGraphs (hereafter TSG) mounted onboard the SA Agulhas-I and SA Agulhas-II research vessels provided
61 high resolution measurements (conductivity, temperature, salinity) along the cruise tracks. The TSG system (Figure 1)
62 is a continuous underway monitoring system connected to a dedicated scientific seawater supply. A conductivity cell
63 measures the conductivity of the seawater pumped in, from which salinity can be deduced, while a thermistors cell
64 measures the temperature of the surface water (which can be combined with the conductivity to infer a value of the
65 water density). An additional temperature sensor is installed across from the hull water inlet for measuring the actual
66 sea surface temperature (SST) before it is slightly modified during seawater way to the conductivity cell. The nominal
67 accuracy of Sea-Bird TSG SSS is better than 0.01 on the practical salinity scale (pss) while the resolution is close to
68 0.001 (www.seabird.com); these values are largely sufficient to capture the surface variability (Gaillard et al., 2015).
69 These sensors are regularly calibrated and continuously monitored in-between cruises, and no appreciable sensor drift
70 emerged in the study period. Regular comparisons between bottle samples and continuous measurements are also
71 carried out onboard during each scientific voyage. However, several aspects could increase the nominal errors and
72 corrupt the data acquired during part of a cruise, i.e. insufficient flow through the conductivity cell, air bubbles presence
73 in the pipe, fouling contamination. Thus an accurate quality control (QC) of the collected dataset, as well as an eventual
74 comparison with external observations, are strongly recommended; these aspects will be addressed in sections 2 and 3,
75 respectively. Furthermore, it is important to remark that the SA Agulhas-I and SA Agulhas-II TSG systems are
76 generally switched on underway; however, when sailing south of 55°S the presence of seaice could block the scientific



77 water supply, repeatedly, hampering data collection. For this reason, the TSG pumps are turned off before entering the
78 icefield in order to reduce the potential damages to the TSG system and the possible acquisition of bad data.
79 In this paper, TSG data and bottle samples used for validation are described in Section 2, as well as the applied QC
80 methodology. Then, section 3 presents the comparison between the TSG SSS and the other reference datasets. Finally,
81 data record details and conclusions are reported in Section 4.

82 **2 Data and methods**

83 We present here the dataset collected by South African icebreakers SA Agulhas-I and SA Agulhas-II during several
84 research cruises in the southern Atlantic Ocean and in the adjacent Southern Ocean sector between December 2010 and
85 February 2017 (Table 1, Figure 2). For each cruise, the full resolution thermo-salinometer dataset has been processed
86 and undersampled with a median filter over 1-minute interval. The dataset is available at
87 <https://doi.org/10.7289/V56M3545>. We plan to provide updates as soon as further observations will be collected and
88 processed. This archive includes the following variables: time of the acquisition; latitude; longitude; conductivity; SSS;
89 SST; SST at hull (SSTH); seaice flag. It is important to remark that SSS is the actual ocean salinity only if the flow rate
90 to the conductivity cell is sufficient; otherwise, it would represent the salinity of the seawater trapped in the TSG. As for
91 temperatures, please note that SST is the temperature of the water volume inside the TSG while SSTH is the
92 temperature of the ocean at the water intake. These values can be slightly different because of heat exchanges along the
93 seawater way to reach the TSG. Exchanges depend on the flow rate, on the volume of water in the circuit and on the
94 temperature difference between the seawater and the ambient temperature (Gaillard et al., 2015).

95 **2.1 Quality control**

96 The QC of the collected TSG measurements included three main steps, which led to discard about 36 % of acquired
97 observations; statistics are summarized in Table 2. Firstly, an automatic detection of unreliable values was performed
98 using selected threshold criteria on conductivity, SSS and SST values (QC-1). Then, following World Ocean
99 Circulation Experiment (WOCE) principles and NOAA National Center for Environmental Information (NCEI)
100 database requirements, quality flags (good, suspicious, bad, harbour, icefield) were attributed to data based on the
101 analysis of several factors, i.e. the detection of insufficient seawater flow, the contamination by air bubbles and the
102 presence of seaice (QC-2). The episodic reductions in seawater flow were identified on the basis of a large and
103 increasing difference between SST and SSTH while SSS remains nearly constant; a threshold difference of 0.2 °C was
104 used for recognizing bad data (Gaillard et al., 2015). The analysis of the conductivity measurements pointed out the
105 presence of episodic quick decreases to underestimated, and often unreliable, values; of course, this is reflected also on
106 SSS, with variations that range between few decimals and several units on the pss. This phenomenon is due to the
107 presence of air bubbles in the conductivity cell usually associated with strong waves and severe sea state conditions.
108 The effect of air bubbles usually run out in few minutes. Measurements showing evidence of this conductivity decrease
109 were flagged as bad data. Furthermore, information included in the cruise reports was carefully analyzed to be aware of
110 these events and other suspicious malfunctioning of the system. Harbour data and observations collected when sailing
111 into icefields were also flagged at this step, and discarded similarly to all the other bad data.

112 Finally, a visual inspection of individual campaigns was carried out (QC-3), with a specific attention to data flagged as
113 suspicious in the QC-2. An additional 2% of bad measurements were discarded, while suspicious values passing this
114 analysis were set to good. Nevertheless, a seaice flag was included in the dataset for indentifying valid measurements
115 that could have been slightly affected by scattered seaice contamination, as recorded by cruise reports, when sailing the



116 Southern Ocean. Seaice maps retrieved through satellite passive microwave sensors (Spren et al., 2008; Aulicino et al.,
117 2013; 2014) and, when available, SAR (Wadhams et al., 2016; 2018) and thermal infrared (Aulicino et al., 2018)
118 imagery, were used for confirming icefields locations. However, when not discarded, these flagged data do not seem to
119 affect significantly the good agreement between the provided TSG dataset and several independent SSS products (see
120 section 3).

121 It is important to note that some of the conductivity, SST and SSTH values associated with the published SSS
122 measurements are missing (Table 2). We inform the user that the QC-2 described above was not complete for these
123 values, whereas an in-depth visual inspection was performed.

124 **2.2 Validation versus bottle samples**

125 During all SA Agulhas-I and SA Agulhas-II research voyages, ship-based scientific teams collected salinity samples
126 from the uncontaminated underway lab supply usually at each 20-30 nautical miles. These samples were taken in 250
127 ml double cap glass bottles with rubber stoppers and completely filled to minimize evaporative error. In most cases,
128 these independent water samples were analyzed directly on board with a Portasal salinometer 8410A in order to get a
129 potential reference for adjusting the TSG data. Triple Portasal measures of each sample (then averaging) were usually
130 performed on bottle samples to reduce possible errors. Due to severe weather conditions, during some cruises salinity
131 samples were not analyzed onboard but later. Actually, no systematic bias was found, thus no adjustment on TSG
132 measurements was necessary. Figure 3 shows an example of the comparison between the TSG data and the bottled
133 samples analysed with the Portasal during the southward leg of the SANAE 2012 cruise. Only few outliers are present
134 at the start and, mostly, at the end of this leg. The offset between TSG and Portasal salinity values is plotted in Figure 4;
135 the average standard deviation, correcting for the outlier, would result in a $p < 0.01$. Generally, we found an excellent
136 correlation between the TSG system and the bottled samples with an error rate of about 8%. This is most likely due to
137 the TSG careful maintenance on board the SA Agulhas-I and SA Agulhas-II provided by the scientific teams, including
138 the tank, pump and conductivity cell cleaning at the beginning of each cruise, the TSG stopping when entering the
139 icefield, the possible bio-fouling constant monitoring during the cruise.

140 **3 Comparison of TSG sea surface salinities to other reference datasets**

141 For a general assessment of our measurements, the TSG SSS dataset were compared to several global gridded reference
142 SSS dataset over the Southern Atlantic and the adjacent sectors of the Southern Ocean covered by the South African
143 cruises. The reference datasets, which do not include South African TSG information, are: i) the World Ocean Atlas
144 2013 (WOA13), ii) the Global ARMOR3D L4 products and iii) the GLORYS Ocean Reanalysis. A point-to-point
145 comparison with Argo measurements was also attempted, but the number of co-located observations was found
146 insufficient.

147 WOA13 is a long-term set of objectively analyzed climatologies at annual, seasonal and monthly scale produced by
148 National Oceanic and Atmospheric Administration's National Oceanographic Data Center (NOAA-NODC). We used
149 monthly composite salinity fields on a $\frac{1}{4}$ degree grid (Zweng et al., 2013) for a comparison with our TSG-SSS data. All
150 WOA13 climatological mean fields are available on the NODC website (www.nodc.noaa.gov) in NetCDF as well as
151 other common formats. ARMOR3D is a monthly objective reanalysis that includes salinity on a $\frac{1}{4}$ degree regular grid
152 on 33 depth levels (also at a weekly period in V4). ARMOR L4 products are obtained by assimilating satellite and in
153 situ observations through statistical methods around a climatology. In particular, the ARMOR3D temperature-salinity
154 (T/S) combined fields are generated using a two steps procedure: synthetic fields are obtained from sea level anomalies



155 and SST satellite information projected onto the vertical using a multiple linear regression method and the covariances
156 deduced from historical observations; then, the synthetic fields and all available in-situ T/S profiles (including Argo and
157 CTDs profiles) are combined through an optimal interpolation method (Guinehut et al., 2012). ARMOR3D data are
158 available through the Copernicus online catalogue (marine.copernicus.eu). GLORYS (V4) is a reanalysis project carried
159 out in the framework of Copernicus Marine Environment Monitoring Service (CMEMS), which produces and
160 distributes daily global ocean reanalysis on 75 levels at eddy permitting resolution ($\frac{1}{4}$ degree). Salinity products are
161 generated through the assimilation (based on a reduced order Kalman filter) of in situ T/S observations (including also
162 sea mammals T/S profiles) using the NEMO dynamical ocean model in the ORCA025 configuration (Ferry et al.,
163 2015). Data are available through the Copernicus online catalogue.

164 The TSG-SSS dataset showed general good agreement to the ensemble of reference datasets (WOA13, ARMOR, and
165 GLORYS), with absolute biases generally lower than 0.1 pss and well within the level of spread found among the
166 references themselves. We were aware that differences due to the small-scale variability filtered out by the gridded
167 products could emerge when comparing local measurements to larger scale and monthly averaged salinity fields.
168 However, even though instances where transect data deviate from the reference ensemble were identified, overall local
169 differences were lower than expected. The standard deviation of the local differences is between 0.1 and 0.2 pss and
170 likely corresponds to mesoscale variability. The austral winter and summer examples reported in Figure 5 show that
171 TSG salinities agree well with gridded references regardless of the season; on the other hand, they suggest that the level
172 of agreement changes with latitude in the study region. In the sub-Antarctic waters, TSG-SSS follows very well the
173 large scale signature of the salinity fronts featured in the gridded products; some deviations are present, presumably
174 related to actual salinity mesoscale and sub-mesoscale structures that the monthly maps cannot resolve. When
175 approaching Antarctic waters and the seaice edge, larger spreads from reference products can be found; but most of the
176 significant deviations disappear when masking the seaice flagged SSS values in the transect data (as in Figure 5). These
177 differences can be ascribed to the presence of scattered seaice, which may influence SSS and/or could affect the TSG
178 nominal functioning; but could be also due to the sparseness of in situ observations at high latitudes in the gridded
179 products. Of particular relevance are the larger biases found between the TSG-SSS and the reference datasets later in
180 2015 (Figure 6a), revealing a signature of surface freshening possibly associated with the low Antarctic seaice extent
181 anomaly of 2016, which the gridded references apparently fail to detect. In this case, the freshening signature captured
182 in the TSG-SSS is effectively supported by bottle validation (Figure 6b), lending it further credibility.

183 **4 Data records and conclusions**

184 TSG data are available to the public in text format through an unrestricted repository at
185 <https://doi.org/10.7289/V56M3545>. Table 3 summarizes the main variables, while the metadata are included in the
186 readme file provided with data on the NOAA-NCEI archive. One file is created for each research cruise. The naming
187 convention is code_YYYY.txt, where: code is a cruise type identification name depending on the cruise
188 objective/enquired area, i.e. SANAE, WINTER, MARION, GOUGH; YYYY is the year when TSG acquisition started.

189 We believe that this exceptional SSS dataset represents a valuable source of high resolution independent and reliable
190 information capable of completing data collected through the existing observing networks (i.e., drifters, ARGO floats,
191 glider fleets), and current state-of-the-art gridded salinity products. A seaice flag helps with its correct use south of the
192 Antarctic polar front. The final goal is enlarging the amount of in situ ocean observations available to the scientific
193 community for addressing several climatic issues. In particular, improving the knowledge of sea surface thermohaline
194 features is one of the most important results to be achieved for advancing studies focusing on climate variability of the



195 Southern Hemisphere. Although Southern Ocean is a key place for atmosphere-ocean interactions at different spatial
196 and temporal scales (Cerrone et al., 2017a; 2017b; Buongiorno Nardelli et al. 2017; Fusco et al., 2018), mesoscale and
197 sub-mesoscale processes acting in the Atlantic sector are still poorly known because of the limited number of available
198 in situ measurements and the coarse accuracy/resolution of the available SSS satellite observations (Boutin et al., 2016).
199 That is particularly true of the Antarctic Circumpolar Current region and its fronts, which are characterized by complex
200 dynamics and intense eddies activity (Cotroneo et al., 2013; Frenger et al., 2015). Furthermore, even though causes
201 have not been firmly defined, several studies pointed out that recent salinity changes in the Southern Ocean are among
202 the most prominent signals of climate change in the global ocean (Böning et al., 2008; Haumann et al., 2016); the
203 freshening signature captured in our TSG-SSS could contribute to this debate (Boutin et al., 2013).
204 In this framework, even though limited in time (i.e., few months per year) and space (i.e., the Atlantic sector of the
205 Southern Ocean), the present TSG SSS dataset represents an uncommon opportunity to partially fill this lack of
206 information, and a valuable tool for improving the reconstruction of density fields in combination with numerical
207 simulations (Chen et al., 2017) and the calibration/validation of SSS satellite observations recently provided by SMOS
208 and Aquarius missions.

209

210 **Acknowledgement**

211 We acknowledge the support of the Department of Environmental Affairs (DEA), South Africa; the South African
212 National Antarctic Programme (SANAP), South Africa; and the Italian National Antarctic Research Programme
213 (PNRA), Italy. This study was made possible thanks to the contribution of the Southern Ocean Choekpoint: an Italian
214 Contribution (SO-ChIC) project and the Multiplatform Observations and Modeling in a sector of the Antarctic
215 circumpolar current (MOMA) project. Special thanks go to the Captain, Officers and crew of the SA Agulhas-I and II as
216 well as all the technicians, scientists and students on board the SA Agulhas-I and SA Agulhas-II research vessels who
217 contributed to the TSG data functioning and cleaning, and to the onboard SSS validation activities.

218

219

220 **References**

221 Ansonge, I.J., Baringer, M.O., Campos, E.J.D., Dong, S., Fine, R.A., Garzoli, S.L., Goni, G., Meinen, C.S., Perez, R.C.,
222 Piola, A.R., Roberts, M.J., Speich, S., Sprintall, J., Terre, T. and van den Berg, M.A.: Basin-wide oceanographic array
223 bridges the South Atlantic, *Eos Trans.*, 95, 53–54, 2014.

224 Aulicino, G., Fusco, G., Kern, S. and Budillon, G.: 1992–2011 sea ice thickness estimation in the Ross and Weddell
225 Seas from SSM/I brightness temperatures, European Space Agency, Special Publication ESA SP-712, 2013.

226 Aulicino, G., Fusco, G., Kern, S. and Budillon, G.: Estimation of sea ice thickness in Ross and Weddell Seas from
227 SSM/I brightness temperatures, *IEEE Trans. Geosci. Remote Sens.*, 52, 4122–4140, 2014.

228 Aulicino, G., Sansiviero, M., Paul, S., Cesarano, C., Fusco, G., Wadhams, P. and Budillon, G.: A new approach for
229 monitoring the Terra Nova Bay polynya through MODIS ice surface temperature imagery and its validation during
230 2010 and 2011 winter seasons. *Remote Sens.*, 10, 366, 2018.

231 Böning, C.W., Disper, A., Visbeck, M., Rintoul, S.R. and Schwarzkopf, F.U.: The response of the Antarctic
232 Circumpolar Current to recent climate change. *Nat. Geosci.* 1, 864–869, 2008.



- 233 Boutin, J., Martin, N., Reverdin, G., Yin, X. and Gaillard, F.: Sea surface freshening inferred from SMOS and ARGO
234 salinity: impact of rain. *Ocean Sci.*, 9, 183–192, 2013.
- 235 Boutin, J., Chao, Y., Asher, W.E., Delcroix, T., Drucker, R., Drushka, K., Kolodziejczyk, N., Lee, T., Reul, N.,
236 Reverdin, G., Schanze, J., Soloviev, A., Yu, L., Anderson, J., Brucker, L., Dinnat, E., Santos-Garcia, A., Jones, W.L.
237 Maes, C., Meissner, T., Tang, W., Vinogradova, N., and Ward, B.: Satellite and in situ salinity: Understanding near-
238 surface stratification and subfootprint variability. *Bull. Amer. Meteor. Soc.*, 97, 1391–1407, 2016.
- 239 Buongiorno Nardelli, B., Guinehut, S., Verbrugge, N., Cotroneo, Y., Zambianchi, E. and Iudicone, D.: Southern Ocean
240 mixed-layer seasonal and interannual variations from combined satellite and in situ data. *J. Geophys. Res.*, 122, 10042–
241 10060, 2017.
- 242 Cerrone, D., Fusco, G., Simmonds, I., Aulicino, G. and Budillon, G.: Dominant covarying climate signals in the
243 Southern Ocean and Antarctic sea ice influence during the last three decades. *J. Clim.*, 30, 3055–3072, 2017a.
- 244 Cerrone, D., Fusco, G., Cotroneo, Y., Simmonds, I. and Budillon, G.: The Antarctic Circumpolar Wave: Its presence
245 and inter-decadal changes during the last 142 years. *J. Clim.*, 30, 6371–6389, 2017b.
- 246 Chen, J., Zhang, R., Wang, H., Yuzhu, A., An, Y., Wang, L. and Wang, G.: An analysis on the error structure and
247 mechanism of soil moisture and ocean salinity remotely sensed sea surface salinity products. *Acta Oceanol. Sin.*, 33, 48,
248 2014.
- 249 Chen, J., You, X., Xiao, Y., Zhang, R., Wang, G., and Bao, S.: A performance evaluation of remotely sensed sea
250 surface salinity products in combination with other surface measurements in reconstructing three-dimensional salinity
251 fields. *Acta Oceanol. Sin.*, 36, 15, 2017.
- 252 Cotroneo, Y., Budillon, G., Fusco, G., and Spezie, G.: Cold core eddies and fronts of the Antarctic Circumpolar Current
253 south of New Zealand from in situ and satellite data, *J. Geophys. Res. Oceans*, 118, 2653–2666, 2013.
- 254 D'Addezio, J.M. and Subrahmanyam, B.: Sea surface salinity variability in the Agulhas Current region inferred from
255 SMOS and Aquarius, *Rem. Sens. of Environ.*, 180, 440–452, 2016.
- 256 Ferry, N., Parent, L., Masina, S., Storto, A., Haines, K., Valdivieso, M., Barnier, B., Molines, J.M., Zuo, H. and
257 Balmaseda, M.: Product user manual for Global Ocean Reanalysis Products, CMEMS version scope: Version 1.0, 2015.
- 258 Frenger, I., Muennich, M., Gruber, N. and Knutti, R.: Southern Ocean eddy phenomenology, *J. Geophys. Res. Oceans*,
259 120, 7413–7449, 2015.
- 260 Fusco, G., Cotroneo, Y. and Aulicino, G.: Different Behaviours of the Ross and Weddell Seas Surface Heat Fluxes in
261 the Period 1972–2015. *Climate*, 6, 17, 2018.
- 262 Gaillard, F., Diverres, D., Jacquin, S., Gouriou, Y., Grelet, J., Le Menn, M., Tassel, J. and Reverdin, G.: Sea surface
263 temperature and salinity from French research vessels, 2001–2013, *Sci. Data*, 2, 150054, 2015.
- 264 Guinehut, S., Dhomps, A.L., Larnicol, G. and Le Traon, P.Y.: High resolution 3D temperature and salinity fields
265 derived from in situ and satellite observations, *Ocean Sci.*, 8(5), 845–857, 2012.



- 266 Haumann, F.A., Gruber, N., Münnich, M., Frenger, I. and Kern S.: Sea-ice transport driving Southern Ocean salinity
267 and its recent trends, *Nature*, 537, 89–92, 2016.
- 268 Helm, K.P., Bindoff, N.L. and Church, J.A.: Changes in the global hydrological-cycle inferred from ocean salinity.
269 *Geophys. Res. Lett.* 37, L18701, 2010.
- 270 Kerr, Y., Waldteufel, P., Wigneron, J.P., Delwart, S., Cabot, F., Boutin, J., Escorihuela, M.J., Font, J., Reul, N.,
271 Gruhier, C., Juglea, S., Drinkwater, M., Hahne, A., Martin-Neira, M. and Mecklenburg, S.: The SMOS mission: A new
272 tool for monitoring key elements of the global water cycle, *Proceedings of the IEEE*, 98(5), 666-687, 2010.
- 273 Kohler, J., Sena Martins, M., Serra, N. and Stammer, D.: Quality assessment of spaceborne sea surface salinity
274 observations over the northern North Atlantic, *J. Geophys. Res. Oceans*, 120, 94–112, 2015.
- 275 Lagerloef, G., Boutin, J., Chao, Y., Delcroix, T., Font, J., Niiler, P., Reul, N., Riser, S., Schmitt, R., Stammer, D.,
276 Wentz, F.: Resolving the global surface salinity field and variations by blending satellite and in situ observations, in
277 *Proceedings of the "OceanObs'09: Sustained Ocean Observations and Information for Society" Conference*, vol. 2,
278 2010. Edited by J. Hall, D.E. Harrison and D. Stammer, Eur. Space Agency Publ., Venice, Italy, 21–15 September
279 2009.
- 280 Le Vine, D., Lagerloef, G., and Torrusio, S.: Aquarius and remote sensing of sea surface salinity from space,
281 *Proceedings of the IEEE*, 98(5), 688-703, 2010.
- 282 Rahmstorf, S.: Thermohaline Ocean Circulation. In: *Encyclopedia of Quaternary Sciences*, Ed. by S. A. Elias, Elsevier,
283 Amsterdam, 2006.
- 284 Reul, N., Chapron, B., Lee, T., Donlon, C., Boutin, J. and Alory, G.: Sea surface salinity structure of the meandering
285 Gulf Stream revealed by SMOS sensor, *Geophys. Res. Lett.*, 41, 3141–3148, 2014.
- 286 Sansiviero, M., Morales Maqueda, M.Á., Fusco, G., Aulicino, G., Flocco, D., and Budillon, G.: Modelling sea ice
287 formation in the Terra Nova Bay polynya, *J. Mar. Syst.*, 166, 4-25, 2017.
- 288 Spreen, G., Kaleschke, L. and Heygster, G.: Sea ice remote sensing using AMSR-E 89 GHz channels, *J. Geophys. Res.*,
289 113, C02S03, 2008.
- 290 Tang, W., Yueh, S.H., Fore, A.G. and Hayashi, A.: Validation of Aquarius sea surface salinity with in situ
291 measurements from Argo floats and moored buoys, *J. Geophys. Res. Oceans*, 119, 6171–6189, 2014.
- 292 Wadhams, P., Aulicino, G., Parmiggiani, F. and Pignagnoli, L.: Sea ice thickness mapping in the Beaufort Sea using
293 wave dispersion in pancake ice - A case study with intensive ground truth. European Space Agency, Special Publication
294 ESA SP-740, 2016.
- 295 Wadhams, P., Aulicino, G., Parmiggiani, F., Persson, P.O.G. and Holt, B.: Pancake ice thickness mapping in the
296 Beaufort Sea from wave dispersion observed in SAR imagery, *J. Geophys. Res. Ocean*, 2018.
- 297 World Meteorological Organization: GCOS 2016 Implementation Plan, “The Global Observing System for Climate:
298 Implementation Needs”, 2016.



299 Zweng, M.M, Reagan, J.R., Antonov, J.I., Locarnini, R.A., Mishonov, A.V., Boyer, T.P., Garcia, H.E., Baranova, O.K.,
300 Johnson, D.R., Seidov, D. and Biddle, M.M.: World Ocean Atlas 2013, Volume 2: Salinity, S. Levitus, Ed., A.
301 Mishonov Technical Ed., NOAA Atlas NESDIS, 74, 2013.

302

303 **Tables and Figures**

Cruise Name	Ship	Start Date	End Date	Latitude	Longitude
SANAE 2010	Agulhas-I	08 Dec 2010	10 Feb 2011	33.96 – 70.65 °S	37.00 °W – 15.99 °E
SANAE 2011	Agulhas-I	10 Dec 2011	08 Feb 2012	37.62 – 70.46 °S	36.51 °W – 11.92 °E
Winter 2012	Agulhas-II	09 Jul 2012	01 Aug 2012	33.87 – 57.16 °S	0.00 °E – 43.07 °E
Gough 2012	Agulhas-II	06 Sep 2012	10 Oct 2012	33.92 – 50.25 °S	15.00 °W – 18.09 °E
SANAE 2012	Agulhas-II	07 Dec 2012	19 Feb 2013	33.88 – 70.80 °S	35.77 °W – 18.69 °E
Marion 2013	Agulhas-II	10 Apr 2013	16 May 2013	33.88 – 47.79 °S	18.22 °E – 43.23 °E
Gough 2013	Agulhas-II	05 Sep 2013	12 Sep 2013	34.06 – 37.06 °S	11.89 °W – 18.14 °E
Marion 2014	Agulhas-II	02 Apr 2014	06 May 2014	33.88 – 58.75 °S	18.25 °E – 38.75 °E
Gough 2014	Agulhas-II	04 Sep 2014	07 Oct 2014	33.87 – 49.26 °S	11.01 °W – 18.60 °E
SANAE 2014	Agulhas-II	05 Dec 2014	16 Feb 2015	33.91 – 70.77 °S	35.31 °W – 17.48 °E
Marion 2015	Agulhas-II	09 Apr 2015	15 May 2015	34.44 – 47.75 °S	18.35 °E – 39.37 °E
Winter 2015	Agulhas-II	23 Jul 2015	14 Aug 2015	33.88 – 56.81 °S	0.00 °E – 18.64 °E
Gough 2015	Agulhas-II	04 Sep 2015	06 Oct 2015	33.90 – 47.73 °S	11.72 °W – 18.61 °E
SANAE 2015	Agulhas-II	05 Dec 2015	10 Feb 2016	34.44 – 70.78 °S	35.62 °W – 17.72 °E
Marion 2016	Agulhas-II	08 Apr 2016	16 May 2016	33.87 – 47.77 °S	18.25 °E – 38.75 °E
Winter 2016	Agulhas-II	05 Jul 2016	27 Jul 2016	33.35 – 55.11 °S	0.00 °E – 29.26 °E
SANAE 2016	Agulhas-II	30 Nov 2016	02 Feb 2017	34.05 – 70.78 °S	33.80 °W – 17.64 °E

304 **Table 1. List of scientific cruises between 2010 and 2017 included in the dataset**

305

306

307

Total measurements	929801	
Discarded data after QC-1	242488	26.0 %
Discarded data after QC-2	316391	34.0 %
Discarded data after QC-3	334687	35.9 %
Valid SSS measurements	595114	
Seaice flagged data	45063	7.5 %
Missing COND and SST values	51275	8.6 %
Missing SSTH values	82527	13.8 %

308 **Table 2. Statistics of the Quality Control**

309



310

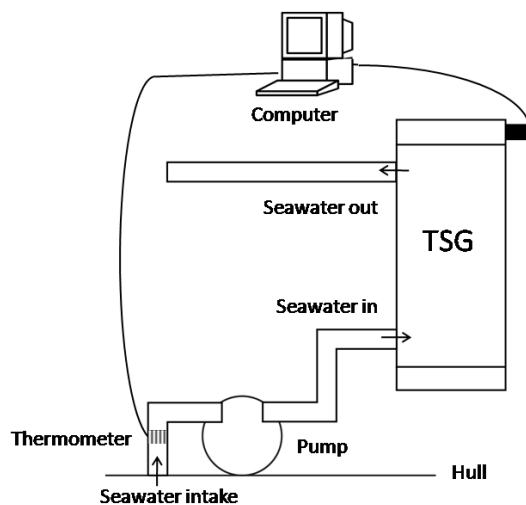
Name of variable	Unit	Description
TIME	dd/mm/yyyyhh:mm	Date and Time of TSG measurement
LAT	Decimal degree	Latitude of TSG measurement
LON	Decimal degree	Longitude of TSG measurement
COND	Siemens / meter	TSG conductivity measurement
SSS	Psu	TSG salinity measurement
SST	Celsius	TSG temperature measurement
SSTH	Celsius	TSG temperature measurement at hull
SEAICE	0 - 1	Seaice flag 0=no ice, 1=scatter ice

311

312 **Table 3. Name and description of the main variables included in the TSG NetCDF files**

313

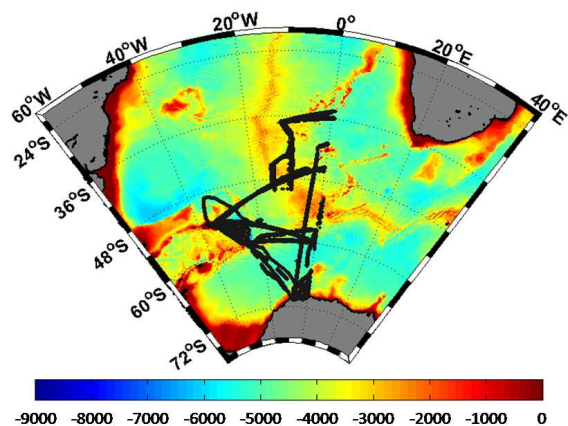
314



315

316 **Figure 1. Schematic of the underway data collection system highlighting the seawater pathway to the conductivity and**
 317 **thermistors cells (TSG), and the temperature sensor location at water inlet.**

318

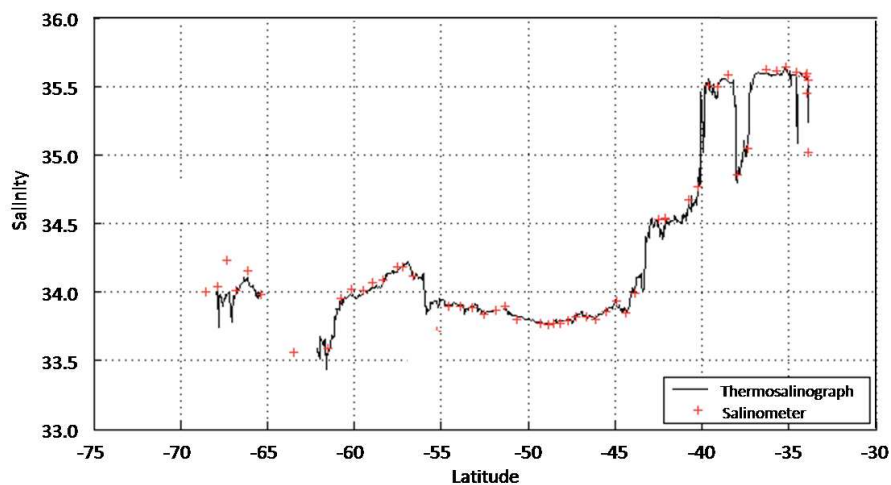


319

320 **Figure 2.** SA Agulhas-I and SA Agulhas-II cruise tracks (black dots) in the southern Atlantic Ocean and in the Southern
321 Ocean between December 2010 and February 2017. Bathymetry is expressed in color.

322

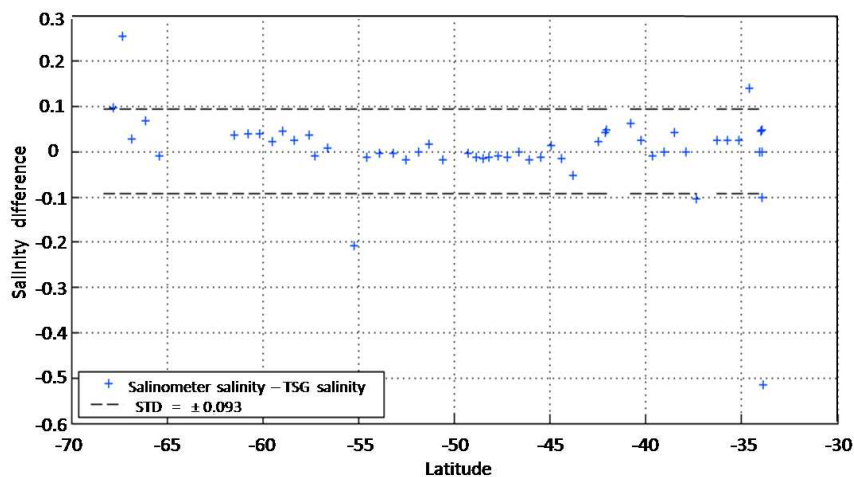
323



324

325 **Figure 3.** A comparison between TSG underway SSS (black line) collected during the southward leg of the SANA E 2012
326 cruise and the related bottle samples measured via the Portasal salinometer (red crosses).

327



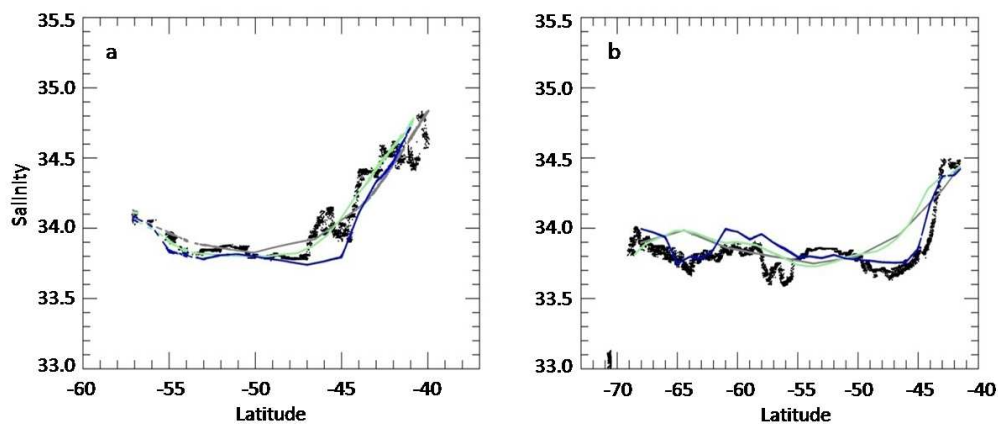
328

329 **Figure 4.** A diagram showing the difference in salinity between the TSG and the Portasal salinometer during the southward
330 leg of the SANA E 2012 cruise. Standard deviation (STD) is reported in the legend box.

331

332

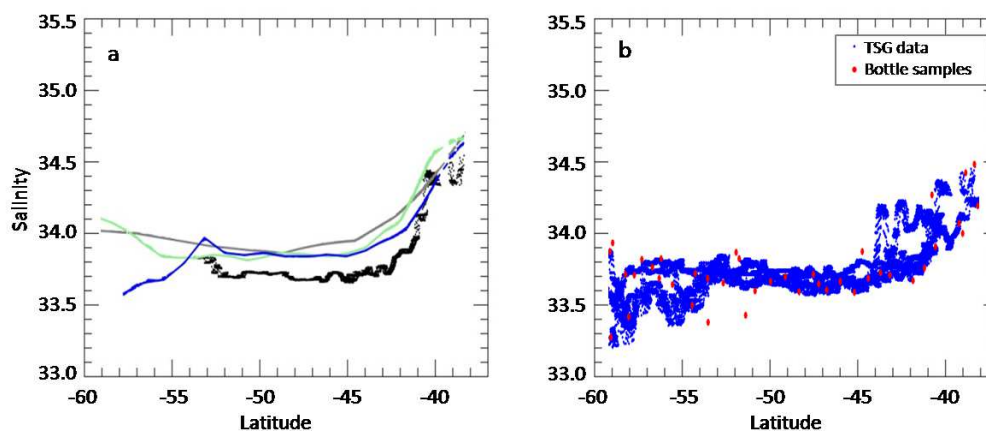
333



334

335 **Figure 5.** A comparison between TSG-SSS (black dots) and monthly gridded products from WOA13 (gray), ARMOR3D
336 (green) and GLORYS (blue) gridded salinities during July 2012 (a) and February 2013 (b) SA Agulhas-II scientific cruises.

337



338

339 Figure 6. Another comparison between TSG-SSS (black) and monthly gridded products from WOA13 (gray), ARMOR3D
340 (green) and GLORYS (blue) gridded salinities during December 2015 Agulhas-II scientific cruises, showing a large negative
341 bias between transect and gridded data over Antarctic waters (a), but which is solidly supported by bottles validation (b).